

Optical methods of the realization of Hilbert transformation*

ANNA MAGIERA, MIECZYSLAW PLUTA

Institute of Physics, Technical University of Wrocław, Wybrzeże Wyspiańskiego 27
50-370 Wrocław, Poland.

The paper deals with the properties of Hilbert transforms realized by application, of coherent optical processor and an incoherent optoelectronic system. The properties of transforms performed optically have been compared with the ideal transform by using three kinds of criteria: i) comparison of realizable kernels of transformation with the ideal one, ii) comparison of Fourier transforms of each transformation, and iii) comparison of the transforms obtained. The usability of coherent and incoherent kind of Hilbert transformation in special cases has been shown.

1. Introduction

Hilbert transformation is a useful instrument in those cases where quantities are described by complex amplitude signal. For example, in physical optics and in description of the current rush [1] it is convenient to handle with complex, so-called analytical signal instead of real physical quantities. An ingenious set-up which is able to realize Hilbert transformation of current function was invented by Gabor (see paper [2]). Conception of the two-dimensional Hilbert transformation realization, by using the coherent optical processor, is presented by SOROKO [3]. The possibility of using the Hilbert transformations in one-dimensional optical system for achieving the effect of super resolution is also mentioned by PAPOULIS [4].

Before starting our considerations on optical possibilities of the Hilbert transformation realization, let us briefly present the properties of this transformation that will be useful in further part of this paper.

Hilbert transform $g(x')$ of complex function $f(x)$ is determined by integral transformation

$$g(x') = \mathcal{F}_H\{f(x)\} = 1/\pi \int_{-\infty}^{+\infty} \frac{f(x)}{x-x'} dx. \quad (1)$$

* This work was carried on under the Research Project M.R. I.5.

The result of Hilbert transformation is identical with that obtained from the convolution of the function $f(x')$ with the function

$$k(x') = -1/\pi x', \quad (2)$$

that is why theorems concerning convolution may be applied to the analysis of the properties of Hilbert transform.

If, in particular, by $F(\omega')$, $G(\omega')$ and $K(\omega')$ we denote the Fourier transforms (FT) of the respective functions $f(x')$, $g(x')$ and $k(x')$, then by virtue of the convolution theorem of FT [1] we obtain

$$g(x') = f(x') * k(x'), G(\omega') = F(\omega')K(\omega'). \quad (3)$$

Based on the formula (2) we can show that

$$K(\omega') = -i/\pi \operatorname{sgn}(\omega'). \quad (4)$$

Thus Eq. (3) may be written in a form

$$G(\omega') = -i/\pi \operatorname{sgn}(\omega')F(\omega'). \quad (5)$$

From the relation (5) applying an inverse FT to the function $G(\omega')$ we obtain the following, alternate to the formula (1), form of the Hilbert transformation of the function $f(x')$:

$$g(x') = -i/\pi \mathcal{F}^{-1}\{\operatorname{sgn}(\omega')\mathcal{F}[f(x')]\} \quad (6)$$

where \mathcal{F} and \mathcal{F}^{-1} – symbols of FT and inverse FT, respectively. In the sequel we shall analyse the possibilities of analogue realizations of Hilbert transformation in incoherent and coherent processors, according to the formulae (1) and (6), respectively.

2. Realization of Hilbert transformation in an incoherent processor

The application of an incoherent space-variant optical processor [5] is justified in cases, where the signal which is to be processed appears in a form of a one-dimensional distribution of incoherent light, or it may be easily transformed to such a form (e.g., variable electric runs).

Let $f(x)$ denote a one-dimensional incoherent optical signal. Its Hilbert transform $g(x')$ is determined from the formula (1)

$$g(x') = 1/\pi \int_{-\infty}^{+\infty} \frac{f(x)}{(x-x')} dx. \quad (7)$$

In the sequel the result of the above mathematical operation will be called an ideal Hilbert transform of the function $f(x)$. As far as an optical realization of formula (7) is concerned, the version of incoherent processor (shown in paper [5]) performing convolution of the function of one variable could be applied. A direct application of this system to the realization of an ideal Hilbert transformation is, however, not possible due to three following reasons:

- i) kernel of transformation possesses positive and negative parts,
- ii) values of transformation kernel in the vicinity of zero tend to infinity,
- iii) integration limits are infinite.

The two first conditions cannot be satisfied due to the limitation of the transmittance of photographic material, on which the distribution of transformation kernel must be registered in the interval $(0, 1)$. The third condition

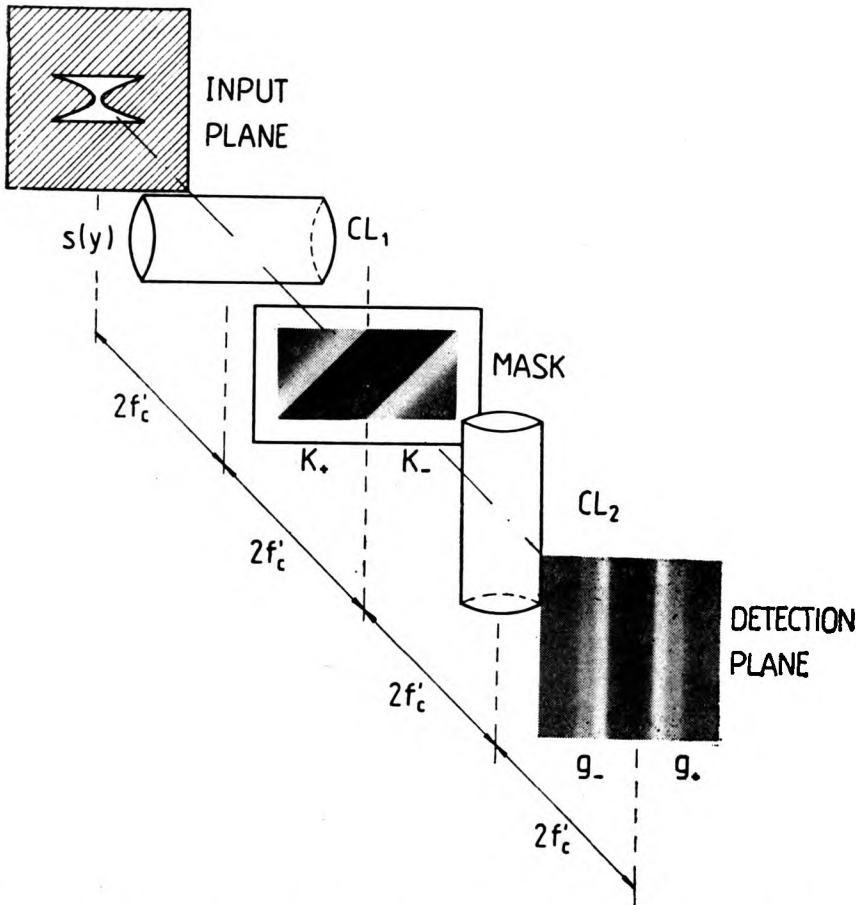


Fig. 1. Scheme of a two-channel incoherent optical processor for realization of Hilbert transformation: $S(y)$ —model of an input function, K_+ , K_- — positive and negative parts of the kernel, respectively, g_+ , g_- — positive and negative parts of the result, respectively, CL_1 , CL_2 — cylindrical lenses, f'_c — focal length of the cylindrical lenses

is not realizable because of the limited transversal dimensions of the optical system and the filter. First limitation may be omitted by constructing a two-channel system in which the positive and negative parts of transformation are performed parallelly and the difference between the results of these operations are measured on the exit (Fig. 1). The choice of a kernel, resembling in shape the ideal one, but with values limited to the interval $(-1, 1)$ gives us possibility of neglecting the second limitation and obtaining the results approximating the ideal ones.

Four curves representing filters used for the transformations, and compared in further part of the paper with an ideal kernel, are shown in Fig. 2.

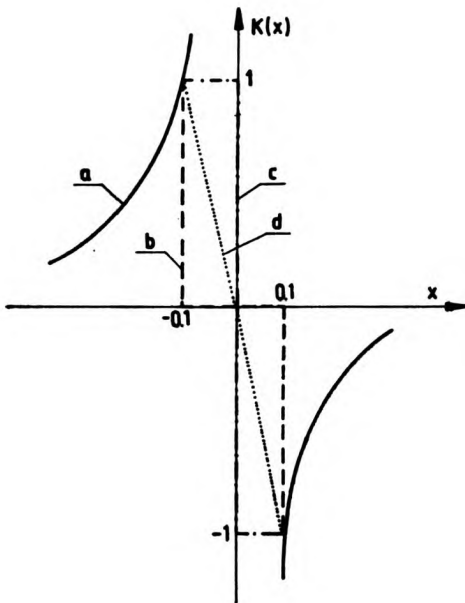


Fig. 2. Transmittances an ideal and real filters

These curves are described by functions:

- a) $k_1(x) = -1/10x,$
 - b) $k_2(x) = -1/10x[1 - \square(5x)],$
 - c) $k_3(x) = -1/10x[1 - \square(5x)] - \square(5x)\text{sgn}(x),$
 - d) $k_4(x) = -1/10x[1 - \square(5x)] - 10\square(5x)x.$
- (8)

Properties of the filters were examined by calculating numerically the transform shapes of the functions: $\square(x/2)$, $x^2\square(x/2)$, $(1-x^2)\square(x/2)$ obtained with the application of those filters. Results are presented in Figs. 3a, b, c. In each of these figures the curve corresponding to the filter $k_3(x)$, (c) is nearest to the ideal transform. The above examples show that the filter, the transmit-

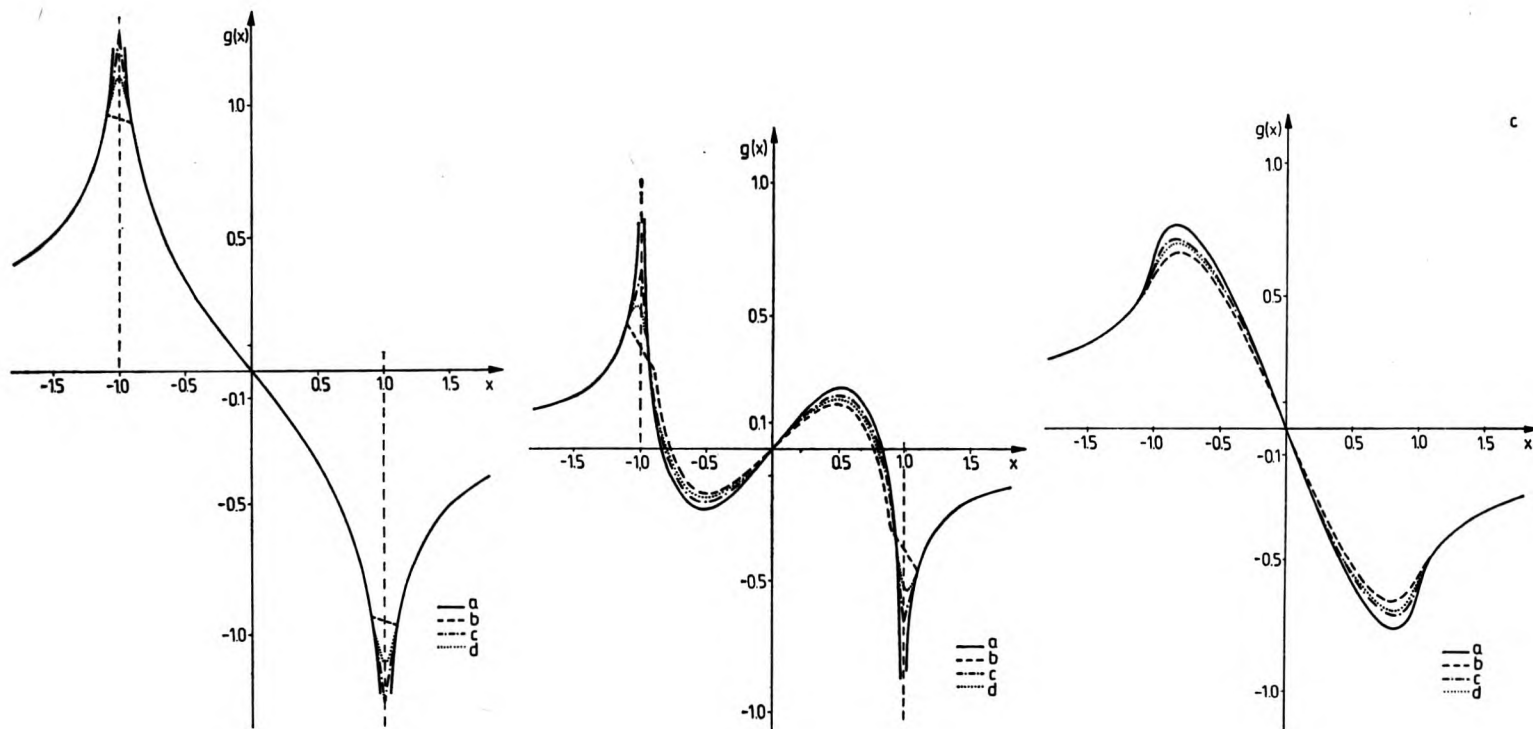


Fig. 3. Calculated results of transforms with the kernels from Fig. 2 for $\square(x/2)$ - a, for $x^2\square(x/2)$ - b, for $(1-x^2)\square(x/2)$ - c

tance of which differs from the value of an ideal kernel for $|x| < 0.1$, well reproduces the shape of Hilbert transformation of functions, the details of which have the dimension orders of unity.

Another way of estimation for real filters is an analytical comparison of special frequencies in real and ideal transforms. Performing a real convolution of the function $f(x)$ with each of the functions of the formula (8) we obtain an ideal $g_1(x')$ and real $g_2(x')$, $g_3(x')$ and $g_4(x')$ transforms, respectively. According to the numeration used in formula (8), we shall denote the Fourier transforms of the kernels of those transformations by $K_1(\omega')$, ..., $K_4(\omega')$, and the Fourier transforms of the results, by $G_1(\omega')$, ..., $G_4(\omega')$. Analogously to the estimation of the imaging systems based on the optical transfer function of frequencies, we shall compare the real transforms, assuming as a standard the frequency spectrum in ideal transforms. Thus the estimation will be based on the function

$$F_{N_i}(\omega) = \frac{G_i(\omega')}{G_1(\omega')}, \quad i = 2, 3, 4. \quad (9)$$

By virtue of the theorem on the Fourier transform of the convolution

$$G_i(\omega') = F(\omega')K_i(\omega'), \quad i = 1, 2, 3, 4 \quad (10)$$

where $F(\omega')$ is the Fourier transform of the object $f(x)$, and substituting (10) into (9) we get

$$F_{N_i}(\omega') = \frac{K_i(\omega')}{K_1(\omega')}, \quad i = 2, 3, 4. \quad (11)$$

Thus we have obtained a criterion which is independent of the transformed function $f(x)$ and depends solely on the shape of the filter $k_i(x)$ to which the function $K_i(\omega')$ is uniquely related. The shapes of functions F_N are shown in Fig. 4. This criterion is also the one to show that the transformation realized

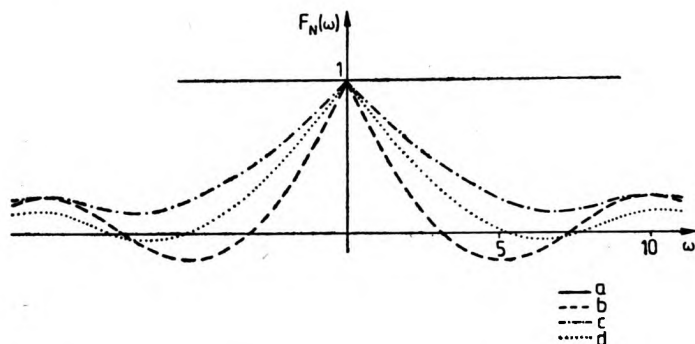


Fig. 4. Normalized frequency spectrum in real transforms to ideal spectrum, $F_N(\omega')$ ratio

by the filter (c) is closest to the ideal transformation, and that high fidelity of the transform can be obtained for the objects the frequencies of which are lower than 1.

When the integration is limited by the boundaries of the filter to $x(-a, a)$ the values of $F_N(\omega')$ decrease tending to zero within the interval $|\omega'| < 1/a$. Thus, the condition iii) may be satisfied approximately by ensuring the integration limits $a \geq 1$. In order to verify the realizability of Hilbert transformation in a noncoherent processor realizing the convolution, the functions $\square(x/2)$, $x^2\square(x/2)$ and $(1-x^2)\square(x/2)$ were recorded experimentally. On this purpose a photographic filter has been produced (Appendix), which corresponds to the case (c), the best one of those examined analytically. This filter was introduced into a mask plane in a two-channel noncoherent processor (Fig. 1). Light intensity distribution was measured in each channel by two, mechanically coupled, detectors, the signal of which was transferred on the "plus" and "minus" inputs of the differential amplifier. The results recorded by an X-Y plotter, and presented in Fig. 5, are similar to those obtained numerically. During the measurements the two-channel processor applied to the realization of Hilbert transformation showed a high sensitivity to the deviations from an ideal adjustment of the system. This sensitivity is due to the operation principle of a two-channel system, where a small value of the Hilbert transform is a difference between two high values of positive and negative parts.

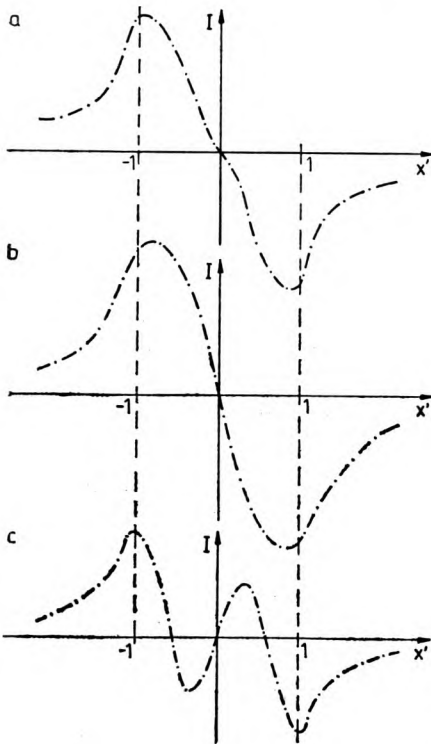


Fig. 5. Results of measurements: for $\square(x/2)$ - a, for $(1-x^2)\square(x/2)$ - b, and for $x^2\square(x/2)$ - c

3. Hilbert transformation in imaging system

Hilbert transformation according to the formula (6) may be realized when using a classic optical coherent processor (realizing two Fourier transformations one after another) with a phase plate in the plane of a spatial filter. It may be also realized in a one-dimensional imaging system with a pupil function $T_H(\xi) = \text{sgn}(\xi)$. In practice, the pupil area is limited by the aperture function $P(\xi)$. For an arbitrary imaging system such a normalization of coordinates in the planes of object, pupil and image is possible that $P(\xi) = 0$ for $|\xi| > 1$, the linear magnification β being equal to unity and propagations of light signal from the object plane to the pupil and from the pupil to the image being described by simple and reverse Fourier transformations (in far-field approximation).

When the coordinates are chosen in this way the amplitude of the complex signal $A'(x')$ of a coherent object $A(x)$ has the distribution

$$A'(x') = \int_{-\infty}^{+\infty} A(x)h(x'-x)dx \quad (11)$$

where h is the Point Spread Function (PSF) depending on the shape of pupil function $T(\xi)$

$$h(x) = \int_{-\infty}^{+\infty} T(\xi)\exp[-2\pi i x \xi]d\xi. \quad (12)$$

For a pupil function described by $P(\xi)$

$$h'(x) = \mathcal{F}_F\{P(\xi)\}. \quad (13a)$$

The image distribution has the form

$$A'(x') = A(x)*h'(x). \quad (13b)$$

Let us notice that the introduction of a phase filter of the transmittance $T_H(\xi)$ into the pupil plane is equivalent to the multiplication of the function $P(\xi)$ by the function $\text{sgn}(\xi)$. The "antiphase" pupil function $T''(\xi)$ obtained in this way determined a new form of point spread function h''

$$h''(x) = \mathcal{F}_F\{T''(\xi)\} = \mathcal{F}_F\{P(\xi)\}*\mathcal{F}_F\{\text{sgn}(\xi)\} = -\frac{i}{\pi}h'(x)*\frac{1}{x} = i\mathcal{F}_H\{h'(x)\}. \quad (14)$$

Point spread function of the system with an antiphase pupil is thus a Hilbert transform of the point spread function with a pupil function $P(\xi)$.

Thus, using the properties of commutation of the convolution operation, it may be also shown that the amplitude $A''(x')$ in a coherent image of the object $A(x)$, obtained by application of an antiphase system is a Hilbert trans-

form of the amplitude distribution $A'(x')$ in the system without a phase shift

$$\begin{aligned}
 A''(x) &= \dot{A}(x) * \dot{h}''(x) = -i/\pi A(x) * [h'(x) * 1/x] \\
 &= -i/\pi [A(x) * h'(x)] * 1/x = i\mathcal{F}_H\{A'(x)\}.
 \end{aligned}
 \tag{15}$$

By applying the Hilbert transformation the relations describing the amplitude distribution in the image of a coherent object for a system with a semiaperture or with the so-called Faucault knife edge [3] may be simplified to such a one in which the function $P(\xi)$ is multiplied by the Heaviside function $H(\xi)$. In this case it may be shown that the point spread function $h_{1/2}(x)$ has the form

$$h_{1/2}(x) = \frac{1}{2} h'(x) + \frac{1}{2} h''(x),
 \tag{16a}$$

which results from the linearity of Fourier transform and from the relation

$$H(\xi) = \frac{1}{2} + \frac{1}{2} \operatorname{sgn}(\xi).
 \tag{16b}$$

Similarly, the amplitude distribution $A_{1/2}(x)$ (in a system with a semiaperture) in the image of the object $A(x)$ obtained from the formula (15) and based

Table

1a	$ \mathcal{F}_F \left\{ \begin{array}{c} \uparrow f(x) \\ \text{---} \square \text{---} \\ \text{---} x \end{array} \right\} = \frac{1}{2} \mathcal{F}_F \left\{ \begin{array}{c} \uparrow \\ \text{---} \square \text{---} \\ \text{---} \end{array} \right\} + \frac{1}{2} \mathcal{F}_F \left\{ \begin{array}{c} \uparrow \\ \text{---} \square \text{---} \\ \text{---} \end{array} \right\} $
	$ \mathcal{F}_F \left\{ \begin{array}{c} \uparrow \\ \text{---} \square \text{---} \\ \text{---} \end{array} \right\} = \operatorname{sinc}(a\omega) + \frac{i}{\omega} [\cos(a\omega) - 1] $
1b	$ \mathcal{F}_F \left\{ \begin{array}{c} \uparrow f(x) \\ \text{---} \square \text{---} \\ \text{---} x \end{array} \right\} = \frac{1}{2} \mathcal{F}_F \left\{ \begin{array}{c} \uparrow \\ \text{---} \square \text{---} \\ \text{---} \end{array} \right\} + \frac{i}{2} \mathcal{F}_{Hi} \left\{ \mathcal{F}_F \left\{ \begin{array}{c} \uparrow \\ \text{---} \square \text{---} \\ \text{---} \end{array} \right\} \right\} $
	$ \mathcal{F}_F \left\{ \begin{array}{c} \uparrow \\ \text{---} \square \text{---} \\ \text{---} \end{array} \right\} = \frac{1}{2} [2 \operatorname{sinc}(a\omega)] + \frac{i}{2} \mathcal{F}_{Hi} \{ 2 \operatorname{sinc}(a\omega) \} $
1c	$ \mathcal{F}_F \left\{ \begin{array}{c} \uparrow f(x) \\ \text{---} \square \text{---} \\ \text{---} x \end{array} \right\} = \frac{i}{2} \mathcal{F}_{Hi} \left\{ \mathcal{F}_F \left\{ \begin{array}{c} \uparrow \\ \text{---} \square \text{---} \\ \text{---} \end{array} \right\} \right\} + \frac{1}{2} \mathcal{F}_F \left\{ \begin{array}{c} \uparrow \\ \text{---} \square \text{---} \\ \text{---} \end{array} \right\} $
	$ \mathcal{F}_F \left\{ \begin{array}{c} \uparrow \\ \text{---} \square \text{---} \\ \text{---} \end{array} \right\} = \frac{i}{2} \mathcal{F}_{Hi} \left\{ \frac{2i}{\omega} [\cos(\omega a) - 1] \right\} + \frac{1}{2} \left\{ \frac{2}{\omega} [\cos(\omega a) - 1] \right\} $

Table (cont.)

2a		$= \frac{1}{2} \mathcal{F}_F \left\{ \begin{array}{c} \uparrow \\ \bigcirc \end{array} \right\} + \frac{1}{2} \mathcal{F}_F \left\{ \begin{array}{c} \uparrow \\ \bigcirc \\ \downarrow \end{array} \right\}$
		$= -\frac{J_1(KR)}{KR} + i \frac{H_1(KR)}{KR}$
2b		$= \frac{1}{2} \mathcal{F}_F \left\{ \begin{array}{c} \uparrow \\ \bigcirc \end{array} \right\} + \frac{i}{2} \mathcal{F}_{Hi} \left\{ \mathcal{F}_F \left\{ \begin{array}{c} \uparrow \\ \bigcirc \end{array} \right\} \right\}$
		$= -\frac{1}{2} \left[\frac{2J_1(KR)}{KR} \right] + \frac{i}{2} \mathcal{F}_{Hi} \left\{ \frac{2J_1(KR)}{KR} \right\}$
2c		$= \frac{i}{2} \mathcal{F}_{Hi} \left\{ \mathcal{F}_F \left\{ \begin{array}{c} \uparrow \\ \bigcirc \\ \downarrow \end{array} \right\} \right\} + \frac{1}{2} \mathcal{F}_F \left\{ \begin{array}{c} \uparrow \\ \bigcirc \\ \downarrow \end{array} \right\}$
		$= \frac{i}{2} \mathcal{F}_{Hi} \left\{ \frac{i2H_1(KR)}{KR} \right\} + \frac{i}{2} \left[\frac{2H_1(KR)}{KR} \right]$

3a		$= \frac{1}{2} \mathcal{F}_F \left\{ \begin{array}{c} \uparrow \\ \text{osc} \end{array} \right\} + \frac{1}{2} \mathcal{F}_F \left\{ \begin{array}{c} \uparrow \\ \text{osc} \\ \downarrow \end{array} \right\}$
		$= -\frac{\pi}{a} \Pi \left(\frac{\pi\omega}{a} \right) + i \ln \left \frac{\omega - a}{\omega + a} \right $
3b		$= \frac{1}{2} \mathcal{F}_F \left\{ \begin{array}{c} \uparrow \\ \text{osc} \end{array} \right\} + \frac{i}{2} \mathcal{F}_{Hi} \left\{ \mathcal{F}_F \left\{ \begin{array}{c} \uparrow \\ \text{osc} \end{array} \right\} \right\}$
		$= -\frac{1}{2} \left[2 \frac{\pi}{a} \Pi \left(\frac{\pi\omega}{a} \right) \right] + \frac{i}{2} \mathcal{F}_{Hi} \left\{ 2 \frac{\pi}{a} \Pi \left(\frac{\pi\omega}{a} \right) \right\}$
3c		$= \frac{i}{2} \mathcal{F}_{Hi} \left\{ \mathcal{F}_F \left\{ \begin{array}{c} \uparrow \\ \text{osc} \\ \downarrow \end{array} \right\} \right\} + \frac{1}{2} \mathcal{F}_F \left\{ \begin{array}{c} \uparrow \\ \text{osc} \\ \downarrow \end{array} \right\}$
		$= \frac{i}{2} \mathcal{F}_{Hi} \left\{ i2 \ln \left \frac{\omega - a}{\omega + a} \right \right\} + \frac{i}{2} \left[2 \ln \left \frac{\omega - a}{\omega + a} \right \right]$

on linearity of Fourier transform, is described by the formula

$$A_{1/2}(x) = \frac{1}{2}A'(x) + \frac{1}{2}A''(x). \tag{17}$$

The relations (16) and (17) may enable the determination of Fourier transforms of some types of functions. Some examples are given in the Table.

By introducing a phase shift in the aperture the PSF of the system is transformed into its Hilbert transform, but – as shown on the example of the object

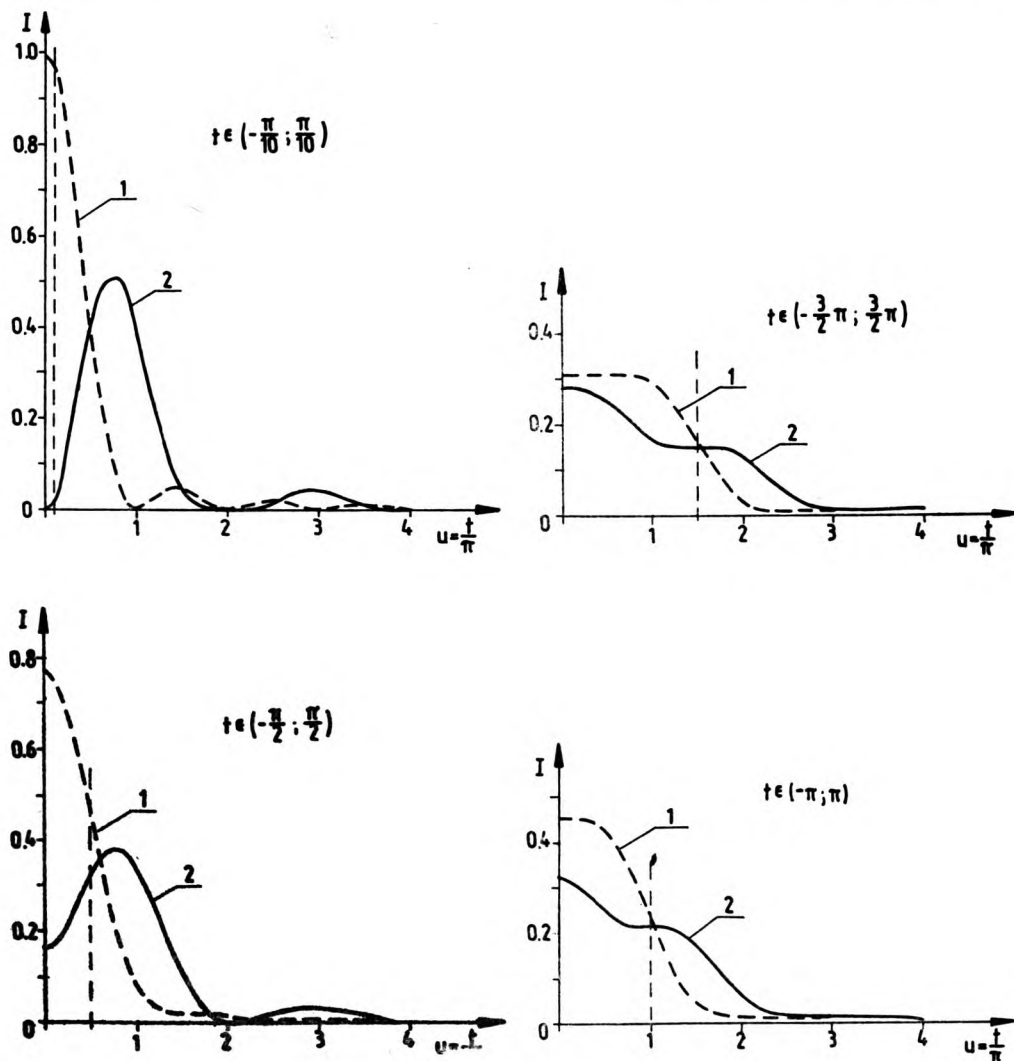


Fig. 6. Images of slits in the system with a pure (1) and antiphase (2) apertures. Edge of the slit is signed by broken vertical line

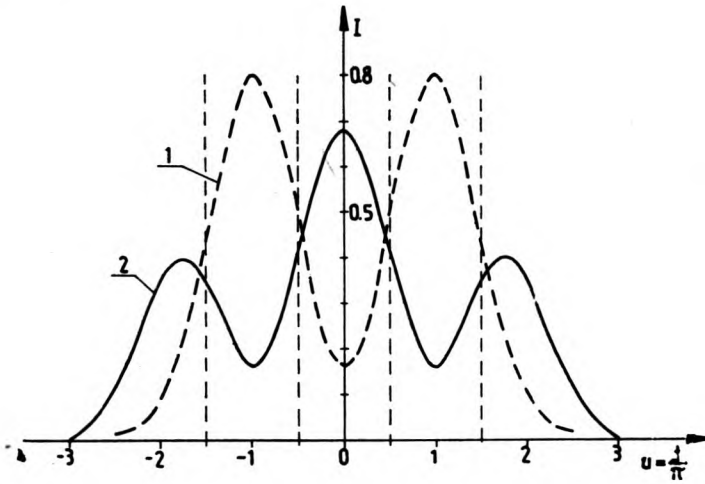


Fig. 7. Images of a pair of slits in the system with a pure (1) and antiphase (2) apertures. Edges of the slits are signed by broken vertical line

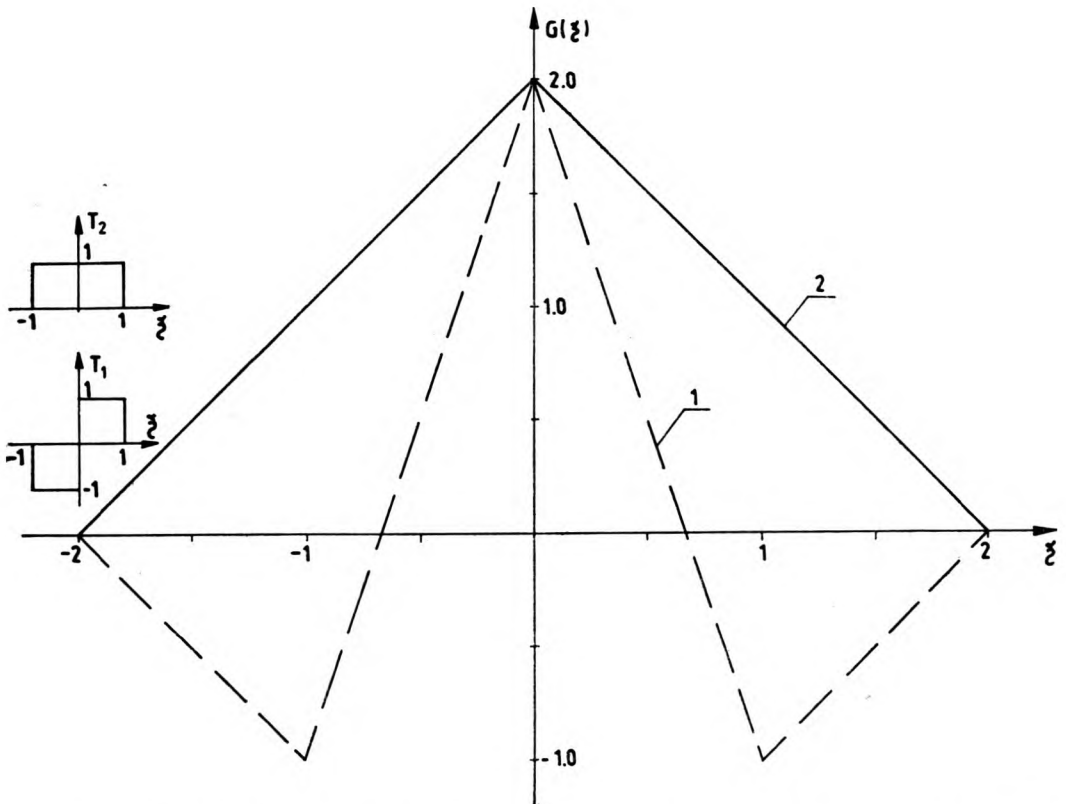


Fig. 8. Transfer function of antiphase aperture (1) contrasted to the pure aperture OTF (2)

in forms of a single slit (Fig. 6a–d) and a pair of slits (Fig. 7) – such an operation does not improve the imaging properties of the system (decrease of contrast and resolution). This conclusion is confirmed by the course of contrast transfer function for an antiphase aperture (Fig. 8).

The fact that phase objects may be visualized with the help of a system with an antiphase aperture, is its advantage. If the amplitude distribution on the input has a phase character, i.e.,

$$A(x) = A_0 \exp i\varphi(x) \quad (18)$$

then, assuming $\varphi(x) \leq 1$, the function $A(x)$ may be written in the following form

$$A(x) \approx A_0 \left(1 + i\varphi(x) - \frac{\varphi^2(x)}{2} \right). \quad (19a)$$

The Hilbert transform of this function has the form

$$\mathcal{F}_H \{A(x)\} = i\mathcal{F}_H \{\varphi(x)\} - \frac{1}{2} \mathcal{F}_H \{\varphi^2(x)\}. \quad (19b)$$

According to the formula (15) the amplitude in the image in antiphase system has the distribution

$$A''(x) = i\mathcal{F}_H \{A(x) * h'(x)\} = A_0 \left(-\mathcal{F}_H \{\varphi(x)\} * h'(x) + \frac{1}{2} i\mathcal{F}_H \{\varphi^2(x)\} * h'(x) \right). \quad (20)$$

Light intensity distribution is

$$I''(x) = A_0^2 \left[(\mathcal{F}_H \{\varphi(x)\} * h'(x))^2 + \left(\frac{\mathcal{F}_H \{\varphi^2(x)\} * h'(x)}{2} \right)^2 \right]. \quad (21)$$

Thus, the light distribution in the image contains information about the object phase.

4. Conclusions

The approximate Hilbert transformation is realizable both in coherent and noncoherent optical processors. Incoherent processor may be helpful, for instance in analysis of electric transients in non-steady states [1]. Its advantage is that the exit signal which has the shape of Hilbert transform may be detected directly. In a coherent system only the square of exit signal modulus may

be recorded, hence, a great uncertainty as to the shape of the transform itself. The application of an antiphase system to visualization of phase object gives the effect described by the formula (21). It is however, worse than that obtained in the method of phase contrast.

Appendix

Photographic recording of the Hilbert transform kernel

The kernel of Hilbert transform is a function of two variables:

$$H(x, x') = \frac{1}{\pi(x-x')}. \quad (\text{A1})$$

In the system of coordinates (SS') turned by $-\pi/4$ we get, however,

$$(x-x') = \sqrt{2}S' \quad (\text{A2})$$

and the two-dimensional function H depends practically on one variable

$$H(SS') = 1/\sqrt{2\pi}S'. \quad (\text{A3})$$

Due to the limitation of intensity transform to the interval $t \in (0, 1)$ the experiment is realized in a two-channel system, applying in each channel an adequately oriented positive part of the function (A3) with constraints of values corresponding to the case (c) discussed in this paper. Thus the transmittance distribution of the positive part of the kernel should be the following

$$t_{H+}(SS') = \begin{cases} 0 & S' < 0 \\ 1 & 0 \leq S' \leq 0.1 \\ \frac{0.1}{\sqrt{2\pi}S'} & S' > 0.1 \end{cases} \quad (\text{A4})$$

The transmittance distribution dependent on one variable may be recorded photographically, applying the system with a cylindric lenses. To this end a non-transparent screen with the aperture of $h(-S')$ width is placed in object plane. After illuminating the screen with a scattered light, the intensity distribution obtained in image plane of the cylindric lens is

$$I(S') \sim h(-S'), \text{ at the magnification of } \beta = -1.$$

The negative photographic process introduces some deformations described by the function τ characterizing the photographic material and processing $t = \tau(Q)$, where t – slide transmittance, Q – illumination. The effect of function τ may be included by introducing suitable corrections to $h(-S')$ and maintaining constant conditions of the slide recording. In our experiment ORWO NP20 films were used, their characteristic τ was first tested and then a pattern of $h(-S')$ made. By employing this pattern in the system with a cylindrical lens a filter corresponding to the function (A4) has been recorded. Such a filter, when turned by $\pi/4$, was placed in the channel realizing the positive part of the transform, and by $-3/4\pi$ in the negative channel (see Fig. 1 – mask plane).

A parallel application of both the filter and two oppositely polarized detectors results in reconstruction of the variant (c) of the Hilbert transform kernel.

References

- [1] BRACEWELL R., *The Fourier transform and its applications* (in Polish), WNT, Warszawa 1968.
- [2] KORPEL A., *Appl. Phys.* **21** (1982), 3624.
- [3] SOROKO L. M., *Holography and coherent optics*, Plenum Press, New York 1980, p. 475.
- [4] PAPOULIS A., *Systems and transforms with application in optics* (in Russian), Mir, Moskva 1971.
- [5] GAJ M., PLUTA M., *Optica Applicata* **11** (1981), 341.

Received May 3, 1984
in revised form July 4, 1984

Оптические методы реализации трансформации Гильберта

Анализируются свойства трансформации Гильберта, реализуемой аналогово в когерентной оптической системе, а также в некогерентном оптоэлектронном процессоре. Произведенные оптические трансформации сопоставлены с идеальной трансформацией при применении трех критериев: сравнения формы ядра реализуемой трансформации с ядром идеальной трансформации, сравнения функции передачи частоты для обеих трансформаций, сравнения форм получаемых трансформант. Указано, кроме того, на полезность трансформаций Гильберта, реализуемых или когерентно, или некогерентно, в зависимости от применения.